

# LIGHT SCATTERING FROM SOOT AGGREGATES WITH RADially INHOMOGENEOUS PRIMARY PARTICLES

T.L. Farias\*, M.G. Carvalho\*, Ü.Ö. Köylü\*\*, G.M. Faeth\*\*\*

\* *Mech. Eng. Dep., Instituto Superior Técnico, 1096 Lisbon, Portugal*

\*\* *Istanbul Tech. Univ., Aeron. and Astron. Faculty, Maslak, Istanbul, Turkey*

\*\*\* *Dep. of Aeros. Eng., The University of Michigan, Ann Arbor, Michigan, 48109-2118, USA*

## ABSTRACT

A study of the scattering of electromagnetic radiation by soot aggregates with spherical primary particles whose optical properties are stratified, i.e., the complex refractive index varies radially from the center to the outer surface, is presented. The ICP algorithm of Iskander et. al [1] was applied to calculate the optical properties of soot aggregates. Numerical simulations were used to construct typical soot aggregates having appropriate fractal properties and prescribed primary particle diameters and number of primary particles per aggregate. Variable complex refractive index within a primary particle was considered using several ICP computational cells per soot primary particle and assuming different refractive indices for the inner and outer cells of each soot primary particle, respectively. This approach was firstly evaluated by computing the scattering properties of sphere-like aggregates, and comparing these results with Mie scattering predictions for an optically equivalent stratified sphere. Optical properties considered included, absorption, differential and total scattering cross sections for aggregates with 48 primary particles and primary particle size parameter,  $x_p$ , of 0.3. Range of aggregate properties for the present study were as follows: ratio between core and coat primary particle size parameter,  $v$ , between 0 and 1, mean fractal dimension,  $D_f$ , of 1.75, and  $|\text{Im}-1|$  ( $m$  = complex refractive index) between 0.2 and 1.4.

## 1. INTRODUCTION

Soot is present within most nonpremixed hydrocarbon-fueled flames, which affects their structure, radiation and pollutant emission. For this reason, the absorption and scattering properties of soot are of interest to estimate continuum radiation from soot and to interpret non

intrusive optical measurements of soot structure and concentrations. Predicting soot optical properties is a challenging task due to the complexity of soot structure and soot composition. Although soot consists of small primary particles that individually satisfy the small particle (Rayleigh) approximation - i.e., the size parameter,  $x_p$ , is much smaller than one for the visible and infrared portion of the spectrum, these particles form branched aggregates that exhibit neither Rayleigh, nor Mie scattering behavior [2-4]. The structure of soot aggregates is rather complex although recent work has shown that they can be treated as mass fractal-like materials, providing useful relationships between their size, namely the radius of gyration, and the number of primary particles they contain [4].

Soot composition can also become a challenging subject if accurate results for the scattering properties of soot particles are desired. Soot primary particle formation process includes the stages of particle generation, whereby the first condensed phase material arises, and particle growth, by which the bulk of the solid phase material is generated [5]. Surface growth involves the attachment of gas phase species to the surface of the particles and their incorporation into the particulate phase. These complex stages are often followed by a phase of soot oxidation in which the soot is burnt in the presence of oxidizing species. It is therefore reasonable to expect that these primary particles are not optically homogeneous but rather have a carbon content and hence a complex refractive index which varies from the surface to the center. Even if this effect is neglected, difficulties in correctly determining the soot complex refractive for different wavelengths have limited the applicability of scattering theories for soot particles. Depending on the experimental or theoretical method adopted, as well as the type of flame and fuel, the real part of the refractive index obtained by different authors varies between 1.4 and 2 while the results of the imaginary part may fall in the range of 0.4 to 1 in the visible and near infrared wavelength ranges (see Ref.[6] and references cited therein).

Although the influence of the complex refractive index in the scattering calculations for soot aggregates has been, to some extent, subject of study in the past [7, 8, 9], the problem of variable refractive index within a primary particle has never been addressed. In order to help fill this gap in the literature, the objective of the present study was to evaluate the influence in the scattering properties of soot aggregates of variable refractive indices within a primary particle.

The paper begins with a brief description of the ICP scattering theory and the method used to numerically simulate aggregates. Evaluation of the method adopted to consider variable complex refractive indices for the core and coat of individual primary particles is then presented. The paper concludes with the evaluation of the influence in the soot scattering properties of variable refractive indices within a primary particle followed by the main conclusions of the present investigation.

## 2. THEORETICAL METHODS

### 2.1 ICP Scattering Theory

Potentially useful approximate theories of soot optical properties that may account for the fractal behavior of soot aggregates have been recently developed [1,3,4,10-14]. One of them, the Rayleigh-Debye-Gans/Fractal-Aggregate theory [3,10,11] has been both theoretically and experimentally evaluated and has proven to be very adequate to correctly predict the scattering properties of complex populations of soot aggregates having widely varying numbers of primary particles per aggregate that should be considered for practical applications [2,15]. Nevertheless this theory assumes that the refractive index of all particles within a single aggregate is constant. Therefore a more exact formulation had to be selected to perform the present investigation.

An extensive comparison of three different solution methods for calculating the extinction and scattering cross sections of agglomerates consisting of assemblies of primary particles in the Rayleigh approximation was presented by Ku and Shim [12], namely the Iskander et al method [1], the Purcell and Pennypacker model [13] and the Jones solution [14]. Although different in their mathematical approaches these three solutions involve the solution of an identical system of linear equations with slightly different coefficients. The main differences between the three approaches reside in the fact that the Jones solution includes multiple scattering terms up to the second order whereas the others include terms up to the third order. The Iskander et al method is the only one that includes a self-interaction term when calculating the electric field induced in each particle. The major conclusions achieved by the authors mentioned above were the following: according to the level of accuracy and range of applicability the ICP solution is the best, followed by the Purcell and Pennypacker and Jones formulation; for the range of validity of the methods (according to the size parameter of the primary particles and absolute value of the refractive index) the ICP method outscores once again its competitors. Following these conclusions, and taking into account that all the three methods require approximately the same amount of computational time and storage, the ICP solution was adopted in the present study.

The solution of the scattering of an electromagnetic wave by an agglomerate of  $N_p$  spherical particles starts by obtaining the internal electric field of each primary particle in the agglomerate due to the incident field, the secondary fields of all the particles surrounding the particle in study and the field of the particle itself. The formulation described below considers ICP cells to be spherical and therefore for the cases where the refractive index within a primary particle is assumed constant it is a common procedure to assume that each primary particle constitutes an ICP computational cell. Nevertheless, in the present investigation the aggregates were studied using

several ICP cells per primary soot particle,  $N_C$ , so that stratified primary particles could be modeled.

The three components of the internal electric field  $E_i$  of the  $i$ th cell can be obtained by solving a linear system of  $3(N_P \times N_C) \times 3(N_P \times N_C)$  equations of the form:

$$E_i = \left( \frac{3}{\epsilon_i + 2} \right) E_{inc,i} + \frac{i}{3} \sum_{\substack{j=1 \\ j \neq i}}^N \left( \frac{\epsilon_j - 1}{\epsilon_j + 2} \right) x_j^3 \bar{T}_{ij} E_j + s_i E_i ; \quad i = 1, 2, \dots, N. \quad (1)$$

Here  $s_i$  is the coefficient of the self-interaction term,  $\epsilon_i = m_i^2$  the dielectric constant and  $\bar{T}_{ij}$  a  $3 \times 3$  matrix in terms of spherical Bessel functions and associated Legendre functions. Once the electric fields inside each cell are known the solution of the scattered wave at any point in the far-field can be obtained. The formulation of ICP is extensive; the corresponding expressions for the differential and total scattering and absorption cross sections can be found in Ref. [12] and references cited therein.

## 2.2 Simulation of Aggregates

In order to correctly use the ICP approach, soot aggregates had to be generated. In the present work, a large sample of aggregates was required, and it was desired that the aggregates have a fractal dimension between 1.7 and 1.85 in order to correspond to recent observations of the fractal properties of soot aggregates [16]. Therefore an alternative to the aggregate simulation method presented by Mountain and Mulholland [17] - where aggregates were generated based on the solution of the Langevin equations - was adopted. The present numerical simulations of aggregates sought to create populations of aggregates by cluster/cluster aggregation, following Jullien and Botet [4]. The process started with individual and pairs of primary particles which then were attached to each other randomly, rejecting configurations where primary particles intersected. This procedure was continued in order to form progressively larger aggregates with the additional restriction that the aggregates should have a fractal dimension between two pre-established limits (1.7 and 1.85 respectively for the present study). It was observed that  $D_f$ , the fractal dimension, fell naturally in the range 1.6-1.9 for the type of aggregates simulated in this study. The fractal dimension of the aggregates produced was verified using the following characteristic relationship of mass fractal aggregates of constant-diameter spherical primary particles between the number of primary particles in the aggregate,  $N_p$ , and the radius of gyration,  $R_g$  [4]:

$$N_p = k_f (R_g/d_p)^{D_f} \quad (2)$$

The fractal dimension and the prefactor,  $D_f$  and  $k_f$ , respectively, appear to be universal properties of soot aggregates. Recent work presented by Koylu et al. [16] indicates  $D_f = 1.83$  and  $k_f = 8.5$  with standard deviations of 0.05 and 0.8, respectively. Projected images of a typical aggregate constructed using the present simulation are illustrated in figure 1.

### 3. RESULTS AND DISCUSSION

#### 3.1 Evaluation of Variable Refractive Index Approach

To model soot aggregates with variable refractive index within primary particles several ICP cell per soot primary particle,  $N_c$ , were used. Depending on the ratio between the core and the coat diameters,  $v$ , different arrangements were tested where the accuracy of the results was analyzed taking into account the computational memory and CPU time required. Among the different structures tested clusters with 9 and 15 ICP cells were selected to model spherical particles with  $v = 0.5$  and  $0.75$  respectively. In both structures the inner cell perfectly matches the core of the equivalent sphere while the outer cells simulate the coat of the sphere. The shape of the outer cells were corrected to fill the void between themselves and the inner cell and the effective refractive indices,  $m_e$ , were calculated using the following Maxwell-Garnett relationship [12]:

$$\left(\frac{m_e^2-1}{m_e^2+2}\right) = f_f \left(\frac{m^2-1}{m^2+2}\right) \quad (3)$$

where  $f_f$  is the filling factor. Geometrical data concerning the two structures adopted are presented in table 1. Present calculations were carried out for  $v = 0, 0.5, 0.75$  and  $1$  and  $|m-1|$  ( $m=n+ik$ ,  $n=1+k$ ) between  $0.2$  and  $1.4$  (which clearly covers the range of values presented for soot refractive indices in the literature in the near infrared and visible parts of the wavelength spectrum). Variation of the refractive index was considered both for the coat and the core assuming in both cases a reference value of  $|m-1| = 0.8$  (leading to  $m=1.56+0.56i$  - a value that is consistent with recent soot aggregate scattering measurements [10]).

Variable Core Refractive index. Predictions of normalized absorption and total scattering cross section as a function of the core refractive index are presented in figure 2a) and 2b) respectively. The coat refractive index was assumed to be constant and equal to the reference value ( $|m_{ct}-1|=0.8$ ). Results also include the case of  $v = 0$  and  $1$  where exact Mie calculations are compared with ICP predictions. Due to the small size of the spherical particle ( $x_p=0.3$ ), which can almost be considered a Rayleigh scatterer, the vertical-vertical ( $vv$ ) scattering patterns are almost constant - variations between forward and back scattering results were less than 5%. Therefore only the  $vv$  scattering cross sections in the forward direction are plotted as function of the core refractive index - see figure 2c. The comparison between the coated sphere results (lines), obtained using a

computer code based on the algorithm presented by Bohren and Huffman [18], and the ICP calculations (symbols) are very encouraging. Throughout the range of refractive indices studied maximum deviations between the two predictions never exceed 5%.

Variable Coat Refractive index. Similar to the previous case, in figure 3 the normalized absorption, total scattering and differential scattering cross sections in the forward direction are presented as a function of the coat refractive index. For the present case the core refractive index was assumed constant and equal to the reference value. Once again, and for the different aspect ratios and refractive indices considered, the differences between the two predictions do not exceed 5%.

Thus, for the range of conditions studied, it has been shown that the approach selected to model the scattering properties of soot aggregates with variable refractive index within a primary particle, although not extremely elegant, seems to be an appropriate one.

### 3.2 Influence of Variable Refractive Index on Soot Scattering Properties

Similar to the study previously presented, the influence of variable refractive index on soot scattering properties was studied by taking  $n = 1+k$  and  $|m-1|$  varying between 0.2 and 1.4. Coat and core refractive indices were varied and the same reference value of  $|m-1|=0.8$  was adopted - corresponding to a typical value for soot in the visible wavelength range [9]. Based on the conclusions of the previous section variable refractive index within soot primary particles were modeled by using 9 and 15 ICP cells per soot primary particle for the cases of  $v = 0.5$  and  $0.75$  respectively.

Results were carried out for aggregates with 48 primary particles and primary particle size parameter of 0.3. Both  $N_p$  and  $x_p$  represent typical values for soot aggregates found in the fuel rich region of laminar flames at wavelengths in the visible part of the spectrum [2]. Larger aggregates capable of representing soot particles in the fuel lean region of sooting diffusion flames [10] could not be studied due to computational limitations - for example, for the case of  $v = 0.75$ , 15 cells per primary particle were used meaning that a system of  $3 \times (48 \times 15) \times 3 \times (48 \times 15)$  had to be solved for each aggregate analyzed. In figure 4 a projected image of a typical simulated aggregate with 1, 9 and 15 ICP cells is shown.

Another issue to be established was the size of soot aggregate population (number of different aggregates and number of orientations of each individual aggregate) that should be averaged in order to obtain statistical significant ICP calculations. For the present conditions ( $x_p=0.3$  and  $N_p=48$ ) the standard deviation of the  $vv$  scattering patterns never exceeded 15%; the maximum values occurring for the larger refractive indices and larger scattering angles. Therefore, 16 different aggregates, each sampled at 4 different orientations were used to obtain a numerical

uncertainty (95% confidence) less than 10% for the ICP predictions of the absorption, total scattering and differential scattering cross sections.

Differential and Total Scattering Cross Section. Normalized vv scattering cross sections for variable refractive indices of the core and coat are illustrated, respectively, in figures 5a) and 5b) as a function of the scattering angle for the most extreme cases considered:  $|m-1| = 0.2$  and  $1.4$ ;  $v$  between 0 and 1. As may be seen the vv scattering cross sections progressively increase as the real and imaginary parts of the refractive index increase varying more than one order of magnitude for the values of  $m$  and  $v$  considered. The results plotted in this figure also clearly show that the influence of the refractive index in the scattering patterns is roughly independent of the scattering angle. Based on this fact, the influence of variable refractive index within the primary particles can be more easily analyzed from the scattering results in a single scattering direction or from the results obtained for the total scattering cross section.

Figure 6a) illustrates the total scattering cross sections normalized by the scattering cross section obtained using the reference value of the refractive index,  $C_{sca}/C_{sca}(|m_{cr, ct}-1|=0.8)$ , as a function of the core refractive index while the coat refractive index was assumed constant. Along the range of  $m$  covered the influence of the core refractive index is reduced for  $v$  up to 0.5. Comparing with the results obtained when constant refractive index within the primary particles is assumed ( $v = 0$ ), maximum deviations roughly exceed 20%. With the increase of the ratio between the core and the coat diameter the influence of the core refractive index becomes more notorious leading, for the limiting case of  $v = 1$ , to deviations of more than 100 %.

In figure 6b) the same results are plotted but for the present case the core refractive index was considered constant while the coat refractive index was varied between the same two limits. As it can be noticed the influence of the core refractive index is almost unnoticed for  $v < 0.5$ . Only for  $v = 0.75$  (where the volume of the core represent 42 % of the total volume of the particle) does the presence of an inner region of the primary particles with a different refractive index become more notorious.

These conclusions, together with the main tendencies of the results presented in figure 6a), suggest that it is the coat refractive index that dominates the scattering patterns of soot aggregates while the existence of a core region with a different refractive index may be neglected if the ratio between the core and the coat diameters is less than 0.5. Additionally, over the range of  $m$  selected, the differential and total scattering cross sections vary over one order of magnitude, highlighting the importance of correctly determining the refractive index of soot and therefore one of the main limitations of accurately estimating the scattering properties of soot aggregates.

Absorption Cross Section. Figure 7 is an illustration of the normalized absorption cross sections as a function of the refractive index for the different aspect ratios studied ( $v=0, 0.5, 0.75$  and  $1$ ). Other parameters of these calculations were similar to figures 5 and 6, namely:  $N_p = 48$ ,  $x_p = 0.3$ ,  $D_f$  between  $1.7$  and  $1.85$  and  $|m-1|$  between  $0.2$  and  $1.4$ .

Figure 7a) illustrate the results obtained when the coat refractive index of the soot primary particles was assumed constant and equal to the reference value. As it may be seen, over the range of refractive indices considered, results obtained for the absorption cross sections are less dependent on the refractive index when compared with the previous case. For  $v$  up to  $0.5$  the core refractive index never produces deviations larger than  $10\%$ . The influence of the core refractive index becomes slightly more notorious as the ratio between core and coat diameters increases. For the limiting case of  $v = 1$ , where the coat vanishes, results obtained for the different values of  $m$  considered may vary by a factor of  $2$ .

In figure 7 b) results obtained considering the core refractive index to be constant and equal to the reference value are plotted as a function of the coat refractive index. Similar to the conclusions obtained for the scattering cross sections, results presented in this figure clearly indicate that the dominant effect on the absorption cross section is the coat refractive index, while the core refractive index only becomes notorious for  $n$  greater than  $0.75$ .

#### 4. CONCLUSIONS

A study of the scattering of electromagnetic radiation by soot aggregates with spherical primary particles whose optical properties are stratified, i.e., the complex refractive index varies radially from the center to the outer surface, was completed where the ICP theoretical approach of Iskander et. al [1] was applied to calculate the optical properties of soot aggregates. Variable complex refractive index within a primary particle was considered using several ICP computational cells per soot primary particle and assuming different refractive indices for the inner and outer cells of each soot primary particle, respectively. Conditions considered during the present investigation were selected to approximate the properties of soot in the visible and near infrared portions of the spectrum. Optical properties considered included, absorption, differential and total scattering cross sections for aggregates with  $48$  primary particles and primary particle size parameter,  $x_p$ , of  $0.3$ . Range of aggregate properties studied were as follows: ratio between core and coat primary particle size parameter,  $v$ , between  $0$  and  $1$  and  $|m-1|$  between  $0.2$  and  $1.4$ . The main conclusions of the study are as follows:

1. - For the range of refractive indices studied in the present work - which covers the typical values for soot particles found in the literature, the scattering cross sections of soot aggregates may



vary by more than one order of magnitude. The coat refractive index seems to dominate the scattering patterns of soot aggregates while the existence of a core region with a different refractive index may be neglected if the ratio between the core and the coat diameters is less than 0.5.

2. - For the absorption cross sections the influence of the refractive index appears to be less notorious. Nevertheless results obtained for the different values of  $m$  considered may vary by a factor of 2. Similar to the conclusions presented for the scattering cross sections, the coat refractive index continues to be the factor that mostly influences the results obtained for the absorption cross sections.

3. - Finally, and based on the previous conclusions, the current uncertainties about the soot refractive index represent the main limitation for accurately estimating the absorption and scattering properties of soot aggregates in flames.

## ACKNOWLEDGMENTS

One of us (T.L.F.) would like to acknowledge the support of the PRAXIS XXI / BD / 2633/94 scholarship. The collaboration between Instituto Superior Técnico and The University of Michigan is sponsored by AGARD Support Project P-101.

## NOMENCLATURE

$C$	- optical cross section [ $m^2$ ]
$d_i$	- diameter of object $i$ [ $m$ ]
$D_f$	- mass fractal dimension [-]
$f_f$	- filling factor, Eq.(3) [-]
$k$	- imaginary part of refractive index of object
$m$	- refractive index of object, $n+ik$
$N_p$	- number of primary particles in an aggregate
$n$	- real part of refractive index of object
$N_c$	- number of ICP cells per soot primary particle
$x_i$	- optical size parameter ( $\pi d_i/\lambda$ ) [-]
$\lambda$	- wavelength of radiation [ $m$ ]
$v$	- ratio between core and coat primary particle diameter [-]
$\theta$	- angle of scattering from forward direction

## Subscripts

abs	- absorption
cr	- core
ct	- coat
e	- optically equivalent object
ICP	- related to ICP calculations
ij	- incident (i) and scattered (j) polarization directions
v	- vertical polarization

## Superscripts

a	- aggregate property
p	- primary particle property
( $\bar{\quad}$ )	- mean value

## REFERENCES

1. M.F. Iskander, H.Y. Chen and J.E. Penner: *Optical Scattering and Absorption by Branched Chains of Aerosols*, Appl. Optics, vol. 28, pp. 3083-3091 (1989).
2. Ü.Ö. Köylü and G.M. Faeth: *Structure of Overfire Soot in Buoyant Turbulent Diffusion Flames at Long Residence Times*, Combust. and Flame, vol. 89, pp. 140-156 (1992).
3. R.A. Dobbins and C.M. Megaridis: *Absorption and Scattering of Light by Polydisperse Aggregates*, Appl. Optics, vol. 30, pp. 4747-4754 (1991).
4. R. Jullien and R. Botet: *Aggregation and Fractal Aggregates*, World Scientific Publishing Co., Singapore (1987).
5. B.S. Haynes and Gg. Wagner: *Soot Formation*, Progr. Energy Comb. Sci., vol. 7, pp. 229-273 (1981).
6. H. Chang and T.T. Charalampopoulos: *Determination of the Wavelength Dependence of Refractive Indices of Flame Soot*, Proc. R. Soc. Lond. A, vol. 430, pp. 577-591 (1990).
7. T.L. Farias, M.G. Carvalho, Ü.Ö. Köylü and G.M. Faeth: *Computational Evaluation of Approximate Rayleigh-Debye-Gans/Fractal-Aggregate Theory for the Absorption and Scattering Properties of Soot*, Radiative Heat Transfer: Current Research, ASME, HTD, vol. 276, pp. 149-159 (1994).
8. P.J. Coelho, T.L. Farias, J.C.F. Pereira and M.G. Carvalho: *Numerical Predictions of Turbulent Sooting Diffusion Flames*, AGARD - CP - 536, n. 8 (1993).

9. T.T. Charalampopoulos: *Morphology and Dynamics of Agglomerated Particulates in Combustion Systems Using Light Scattering Techniques*, Prog. Energy Comb. Scie., vol. 18, pp. 13-45 (1992).
10. Ü.Ö. Köylü and G.M. Faeth: *Optical Properties of Overfire Soot in Buoyant Turbulent Diffusion Flames at Long Residence Times*, J. Heat Transfer, vol. 116, pp. 152-159, 1994.
11. Ü.Ö. Köylü and G.M. Faeth, *Optical Properties of Soot in Buoyant Laminar Diffusion Flames* J. Heat Transfer, vol. 116, pp. 971-979 (1994).
12. J.C. Ku and K. -H. Shim: *A Comparison of Solutions for Light Scattering and Absorption by Agglomerate or Arbitrarily-Shaped Particles*, J. Quant. Spect. Radiat. Transfer, vol. 47, pp. 201-210 (1992).
13. E.M. Purcell and C.R. Pennypacker: *Scattering and Absorption of Light by Nonspherical Dielectric Grains*, Astrophys. Journal, vol. 186, pp. 705-714 (1973).
14. A.R. Jones: *Electromagnetic Wave Scattering by Assemblies of Particles in the Rayleigh Approximation*, Proc. Roy. Soc. London A , vol. 366, pp. 111-127, (1979).
15. T.L. Farias, M.G. Carvalho, Ü.Ö. Köylü and G.M. Faeth: *Computational Evaluation of Approximate Rayleigh-Debye-Gans/Fractal-Aggregate Theory for the Absorption and Scattering Properties of Soot*, J. Heat Transfer, in press (1994).
16. Ü.Ö. Köylü, G.M. Faeth, T.L. Farias and M.G. Carvalho: *Fractal and Projected Structure Properties of Soot Aggregates*, Comb. and Flame, in press (1994).
17. R.D. Mountain and G.W. Mulholland: *Light Scattering from Simulated Smoke Agglomerates*, Langmuir, vol. 4, pp. 1321-1326 (1988).
18. C.F. Bohren and D.R. Huffmann: *Absorption and Scattering of Light by Small Particles*, Wiley, New York (1983).

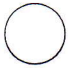







	$v$	ICP Equivalent Structure	$N_c$	$x_{cr, ICP}$	$x_{ct, ICP}$	$m_{cr, ICP}$	$m_{ct, ICP}$
	0		1	0	$x_p$	—	$m_{ct, soot}$
	0.5		9	$0.5 \times x_p$	$0.39 \times x_p$	$m_{cr, soot}$	Eq.3; $f_f = \frac{v}{6}$
	0.75		15	$0.75 \times x_p$	$0.28 \times x_p$	$m_{cr, soot}$	Eq.3; $f_f = \frac{v}{6}$
	1		1	$x_p$	0	$m_{cr, soot}$	—

Table 1. Geometrical data related to the cell structures adopted to model coated spheres with  $v = 0, 0.5, 0.75$  and  $1$ .

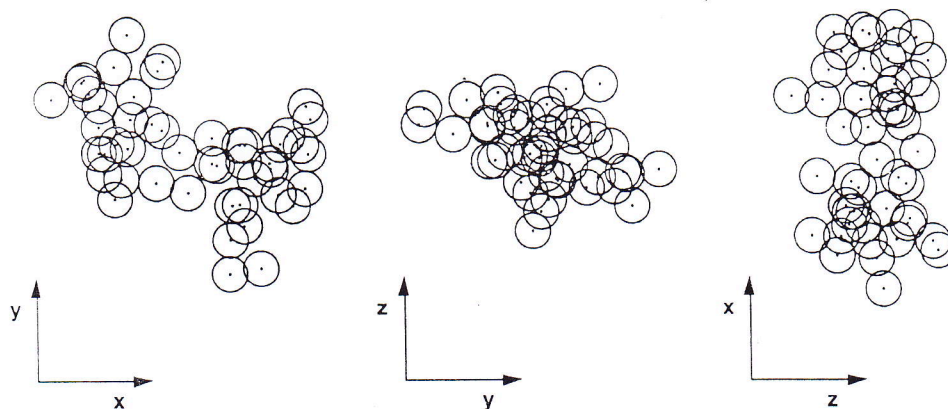


Figure 1. Projected images of a simulated aggregate with 48 primary particles ( $D_f=1.75$ ).

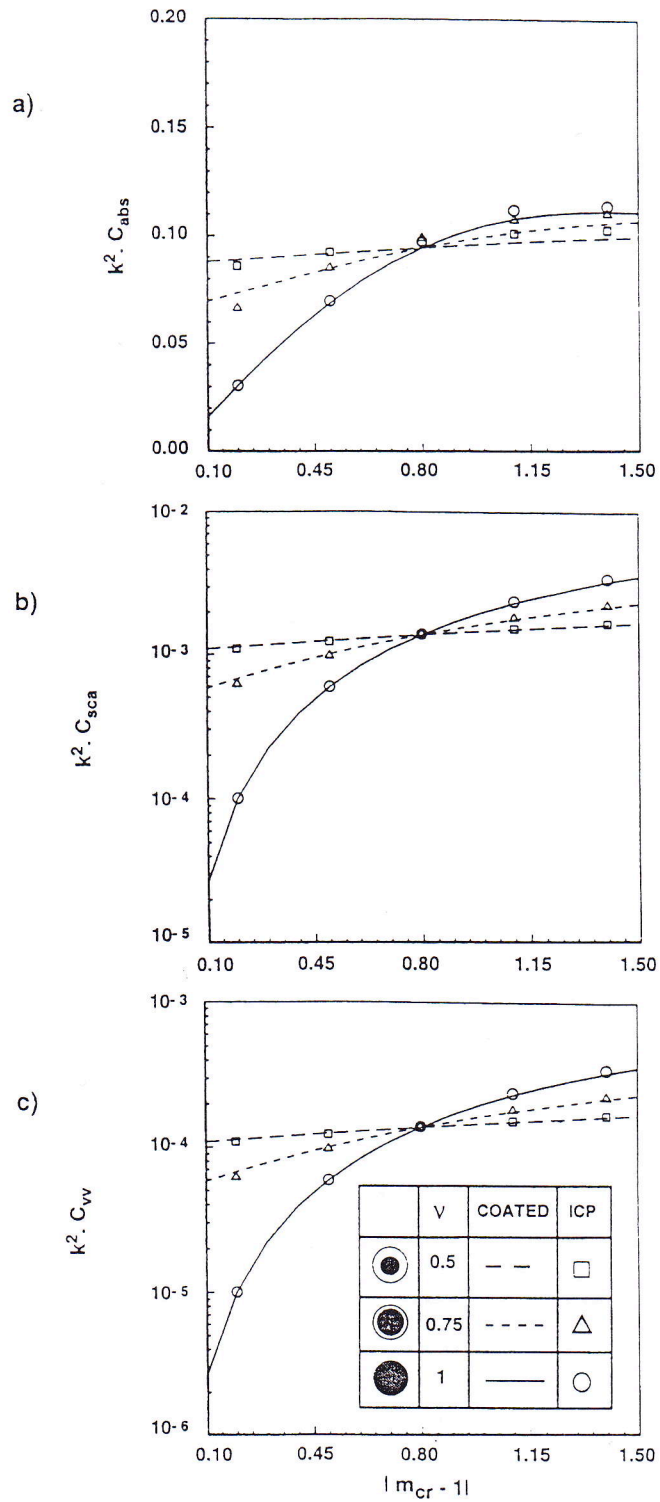


Figure 2. Comparison between coated sphere and ICP predictions as a function of the core refractive index ( $x_p=0.3$ ;  $|m_{ct}-1|=0.8$ ): a) -  $k^2 C_{abs}$ ; b) -  $k^2 C_{sca}$ ; c) -  $k^2 C_{vv}(\theta=0)$ .

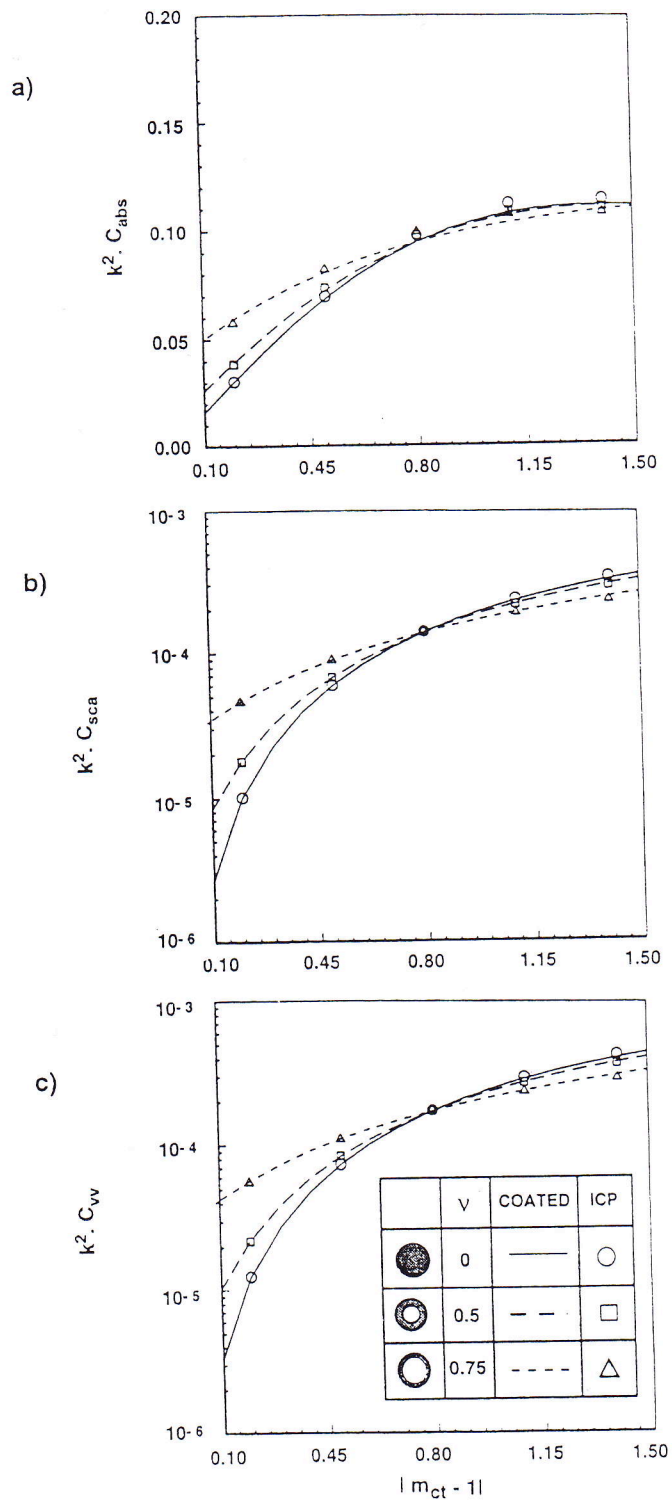


Figure 3. Comparison between coated sphere and ICP predictions as a function of the coat refractive index ( $x_p=0.3$ ;  $|m_{\text{cr}} - 1|=0.8$ ): a) -  $k^2 C_{\text{abs}}$ ; b) -  $k^2 C_{\text{sca}}$ ; c) -  $k^2 C_{\text{vv}}(\theta=0)$ .

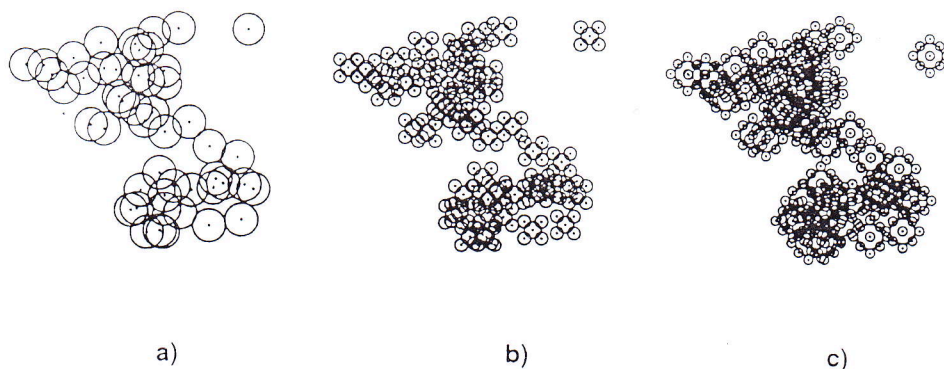


Figure 4. Projected images of an aggregate with 48 primary particles: a)  $N_c=1$ ; b)  $N_c=9$ ; c)  $N_c=15$ .

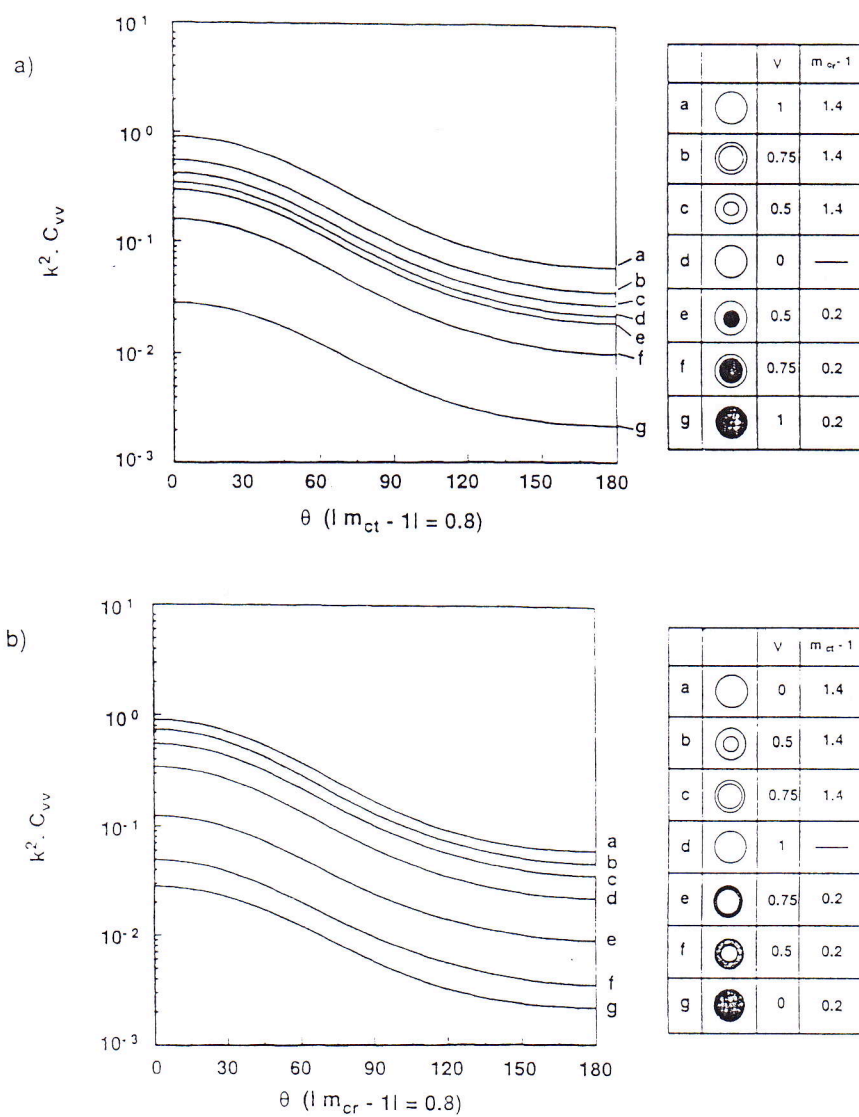


Figure 5. Normalized  $vv$  scattering cross sections as a function of the scattering angle for  $v = 0, 0.5, 0.75$  and  $1$ ;  $N_p = 48$ ,  $x_p = 0.3$ : a) - variable core refractive index ( $|m_{cr} - 1| = 0.2$  and  $1.4$ ); b) - variable coat refractive index ( $|m_{cr} - 1| = 0.2$  and  $1.4$ ).

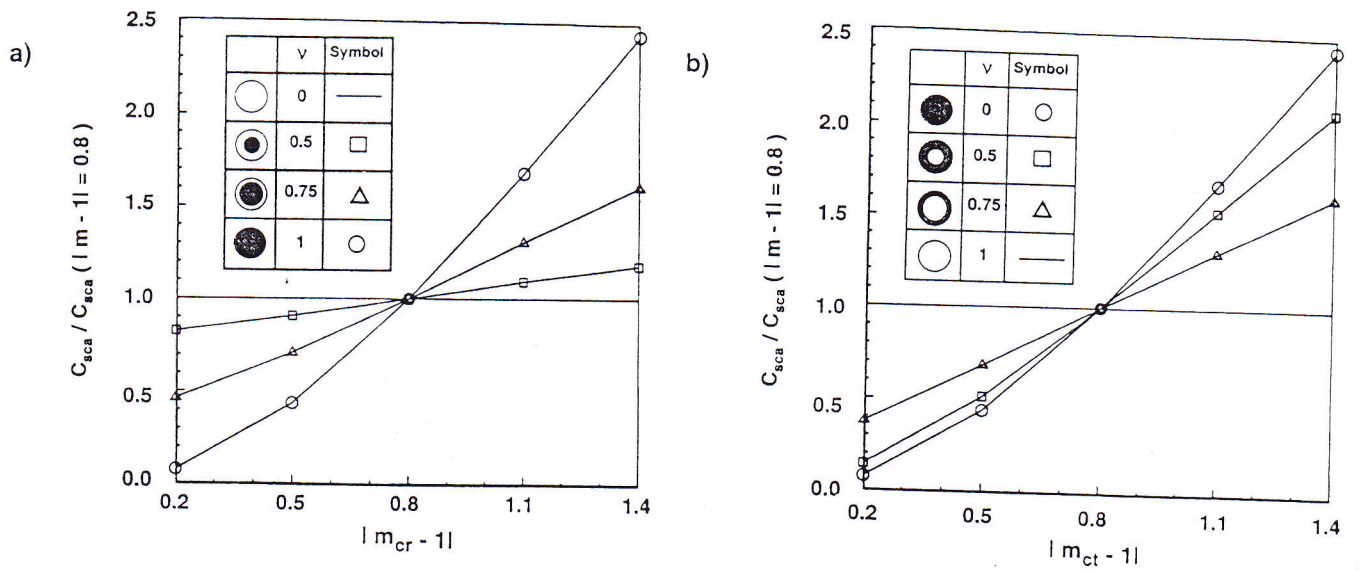


Figure 6. Normalized total scattering cross sections as a function of: a) - the core refractive index ( $|m_{ct}-1| = 0.8$ ); b) - the coat refractive index ( $|m_{cr}-1| = 0.8$ ), for  $v = 0, 0.5, 0.75$  and  $1$ ;  $N_p = 48$  and  $x_p = 0.3$ .

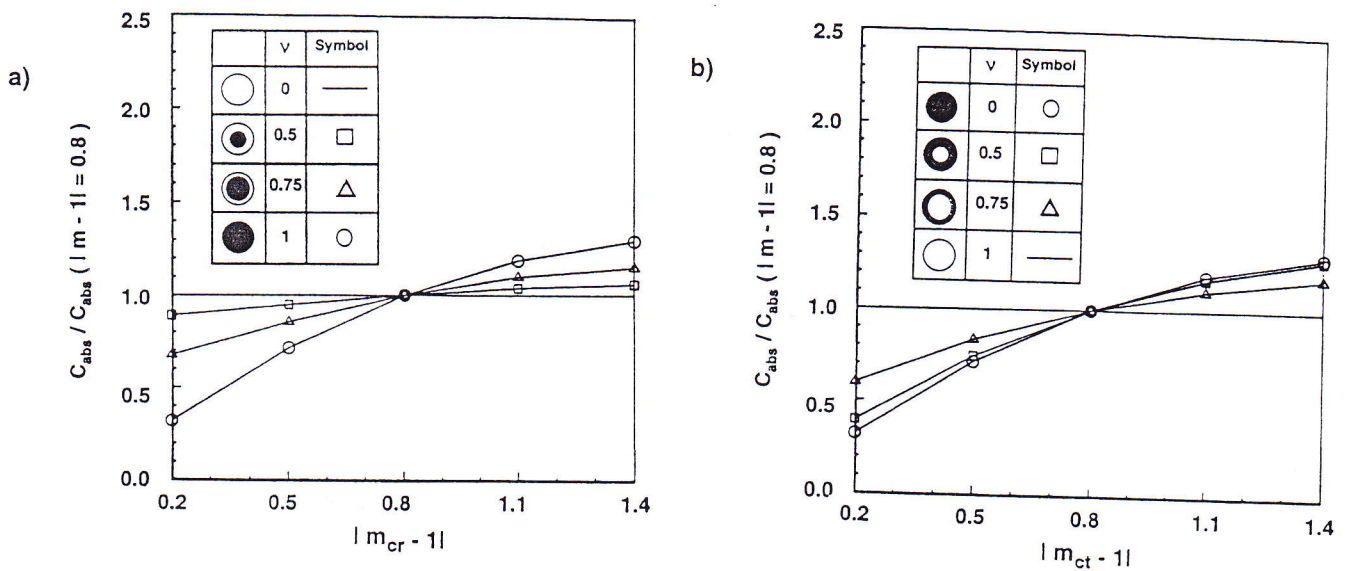


Figure 7. Normalized absorption cross sections as a function of: a) - the core refractive index ( $|m_{ct}-1| = 0.8$ ); b) - the coat refractive index ( $|m_{cr}-1| = 0.8$ ), for  $v = 0, 0.5, 0.75$  and  $1$ ;  $N_p = 48$  and  $x_p = 0.3$ .